Phase Morphology of PP/COC Blends

Miroslav Šlouf,[1] Jan Kolařík,[1] Luca Fambri[2]

[1]*Institute of Macromolecular Chemistry of the Academy of Sciences of the Czech Republic, Heyrovsky sq. 2, 16206 Praha 6, Czech Republic*
[2]*Department of Materials Engineering, University of Trento, via Mesiano, 38050 Trento, Italy*

Received 17 October 2002; accepted 20 April 2003

ABSTRACT: Phase morphology of polymer blends PP/COC, where PP is polypropylene and COC is a copolymer of ethene and norbornene, was characterized by means of scanning electron microscopy (SEM) and scanning transmission electron microscopy (STEM). PP/COC blends were prepared by injection molding and their morphology was studied for six different compositions (90/10, 80/20, 70/30, 60/40, 50/50, and 25/75 wt %). The intention was to improve PP properties by forming COC cocontinuous phase, which should impart to the PP matrix higher stiffness, yield stress, and barrier properties. Surprisingly enough, all studied blends were found to have fibrillar morphology. In the 90/10, 80/20, and 70/30 blends, the PP matrix contained fibers of COC, whose average diameter increased with increasing COC fraction. In the 60/40 blend, the COC component formed in the PP matrix both fibers and larger elongated entities with PP fibers inside. The 50/50 blend was formed by COC cocontinuous phase with PP fibers and PP cocontinuous phase with COC fibers. In the 25/75 blend, PP fibers were embedded in the COC matrix. In all blends, the fibers had an aspect ratio at least 20, were oriented in the injection direction, and acted as a reinforcing component, which was proven by stress–strain and creep measurements. According to the available literature, the fibrous morphology formed spontaneously in PP/COC is not common in polymer blends. J Appl Polym Sci 91: 253–259, 2004

Key words: polypropylene; norbornene; polyolefins; polymer blends; fibrous morphology

INTRODUCTION

Amorphous ethene-norbornene copolymers obtained with metallocene-based catalysts[1,2] rank among new polymer materials with remarkable properties, such as a high glass transition temperature (T_g), transparency, heat resistance, chemical resistance to common solvents, low moisture uptake, high water barrier, good mechanical properties, etc. Available products—usually denoted as cycloolefin copolymers (COC)—have recently attracted much attention in the field of basic and applied material science.[3–9] Glass transition temperature (T_g) of COC is proportional to the norbornene fraction, but no linear correlation has been found.[6] It is so because T_g of COC also depends on microstructure of the backbones: in the case of copolymers made up of predominantly alternating ethylene and norbornene units, the observed T_g was low; higher T_g's have been found for copolymers with long norbornene sequences accounting for enhanced stiffness of the backbones.[7] Besides, it has also been noted that the stereoregularity of chain segments affects the resulting T_g.[6] Increase in T_g caused by annealing was attributed[5] to the growth of rigid amorphous phase because of short-range ordering of norbornene chain segments; the kinetics of this process was reported to obey an equation similar to that for polymer crystallization. Functionalization[4] of COC is believed to expand future application in the fields of medicine and optical fibers.

Studies of mechanical properties of ethene–norbornene copolymers encompass dynamic mechanical thermal analysis (DMTA),[6,8] stress–strain measurements,[6,9] flexural creep,[9] microhardness,[6] impact strength,[3] etc. DMTA has revealed secondary and main transitions associated with local and segmental motions of copolymer backbones. Although the length of polyethylene sequences is not sufficient for crystallization, the phenomenon of yielding is preserved up to about 40% content of norbornene in the copolymers. A rising percentage of norbornene accounts for an increase in yield or tensile strength and a decrease in strain at yielding and break.[6,9] Although impact strength of COC is adequate for many applications, attempts have been made to increase it by admixing thermoplastic styrene–butadiene–styrene elastomers, which allow optical transparency to be maintained.[3]

Correspondence to: M. Šlouf (slouf@imc.cas.cz).
Contract grant sponsor: Grant Agency of the Czech Republic; contract grant number: 106/02/P029.
Contract grant sponsor: Grant Agency of the Academy of Sciences of the Czech Republic; contract grant number: A4050105.
Contract grant sponsor: Academy of Sciences of the Czech Republic; contract grant number: AVOZ 4050913.

Because of their olefinic character, COC is likely to be compatible with polyolefins (PO) by analogy with other polyolefin binary blends, in which the two components were found thermodynamically miscible or mechanically compatible.[10,11] That is why PO/COC blends could be prepared without special compatibilizers. As an "upgrading" component, COC is expected to impart to PO/COC blends increased stiffness, resistance to creep, barrier properties, etc. To our knowledge, so far no data have been published on such types of polypropylene (PP) blends. The morphological and rheological study[12] of PP blends with hydrogenated oligo(cyclopentadiene), which are used in the packaging industry,[13,14] has shown that the components are miscible up to 30% of the latter. In the first step of our studies, we have selected the system PP/COC with regard to our previous articles,[15–20] dealing with blends of PP. Of available COC products of Ticona,[9] we have used Topas 8007 [i.e., the copolymer with the lowest fraction of norbornene (about 30%), the melt temperature (190–250°C), and the melt flow index (MFI), which displays yielding and relatively high strain at break (10%)]. The objective of this article was to prepare blends with cocontinuous upgrading component COC, which would impart to them enhanced mechanical properties in comparison with PP. Numerous studies[21–25] have shown that a cocontinuous component affects physical properties of blends much more that a dispersed (discontinuous) component. Searching for the critical volume fraction of COC, at which this component assumes (partial) continuity, our interest was mainly focused on the composition interval up to 50% of COC.

EXPERIMENTAL

Materials

Polymers used in this study were PP and amorphous COC. PP Moplen C30G was a product of Basell (Ferrara, Italy) [MFI (230°C, 2.16 kg) = 6 mL/min; density, 0.903 g/cm^3; crystallinity, 52%; T_g = −10°C]. The amorphous COC copolymer produced under the trade name Topas 8007 was a product of Ticona (Celanese, Frankfurt, Germany), consisting of 35% of norbornene and 65% of ethene units [MFI = 1.7 g/10 min (190°C, 2.16 kg); density, 1.02 g/cm^3; T_g = 75°C].

Blend preparation

A series of PP/COC blends was prepared with 5, 10, 15, 20, 25, 30, 40, 50, and 75 wt % of COC. Polymers were mixed in a Banbury mixer (chamber 4.3 L; 164 rpm) at 190°C for 3.5 min. Produced pellets were used for feeding a Negri–Bossi injection molding machine (temperature of the melt: 230°C; barrel temperature: 215°C; injection pressure: 30 MPa) to produce dumbbell test specimens ISO 527 (length: 170 mm; thickness: 4 mm; gauge length: 80 mm; gauge width: 10 mm).

Scanning electron microscopy

Scanning electron microscope (SEM) JSM 6400 (Jeol) was used for studying the phase morphology. All samples were fractured in liquid nitrogen parallel and perpendicular to the injection direction. The samples were covered with platinum by using a vacuum sputter coater (SCD 050, Balzers) before being examined in the electron microscope. All SEM micrographs were secondary electron images taken at an acceleration voltage of 25 kV.

Scanning transmission electron microscopy

Scanning electron microscope with a transmission adapter (STEM) Vega TS 5130 (Tescan) was used for studying the phase morphology of the 80/20, 70/30, and 60/40 PP/COC blends. Ultrathin sections for STEM were prepared as follows: small truncated pyramids for ultramicrotoming were cut off from the dumbbell specimens so that their upper face was perpendicular to the injection direction. The pyramids were fixed in ultramicrotome with cryoattachment (Ultrotome III, LKB, and Leica Ultracut UCT). The ultrathin sections were cut from the upper face of the pyramids at −130°C. Microtomed ultrathin sections were then placed on Cu grids and stained in RuO_4 vapors. Ruthenium tetraoxide was prepared by reacting $RuCl_3 \cdot xH_2O$ with NaClO as described in the literature.[26] Best results for PP/COC blends were achieved for 100-min-long staining. Under these conditions, STEM micrographs showed light PP matrix with dark COC particles. All STEM micrographs were taken at an acceleration voltage of 30 kV.

Image analysis

Dimensions of the particles of dispersed components were estimated from several SEM and STEM micrographs with the micrometer scale. In most blends studied in this work, the COC minority component formed fibers in the PP matrix. Fiber diameters were determined by using several hundreds of fibers in both SEM and STEM micrographs. The accuracy of fiber length evaluation was limited as discussed below. Nevertheless, it was possible to estimate the length of a few COC fibers by using SEM micrographs of fracture surfaces parallel to the injection direction.

Stress–strain measurements

An Instron tester, type 4502, was used to measure tensile mechanical properties of studied blends at about 23°C. Tensile modulus was determined by using

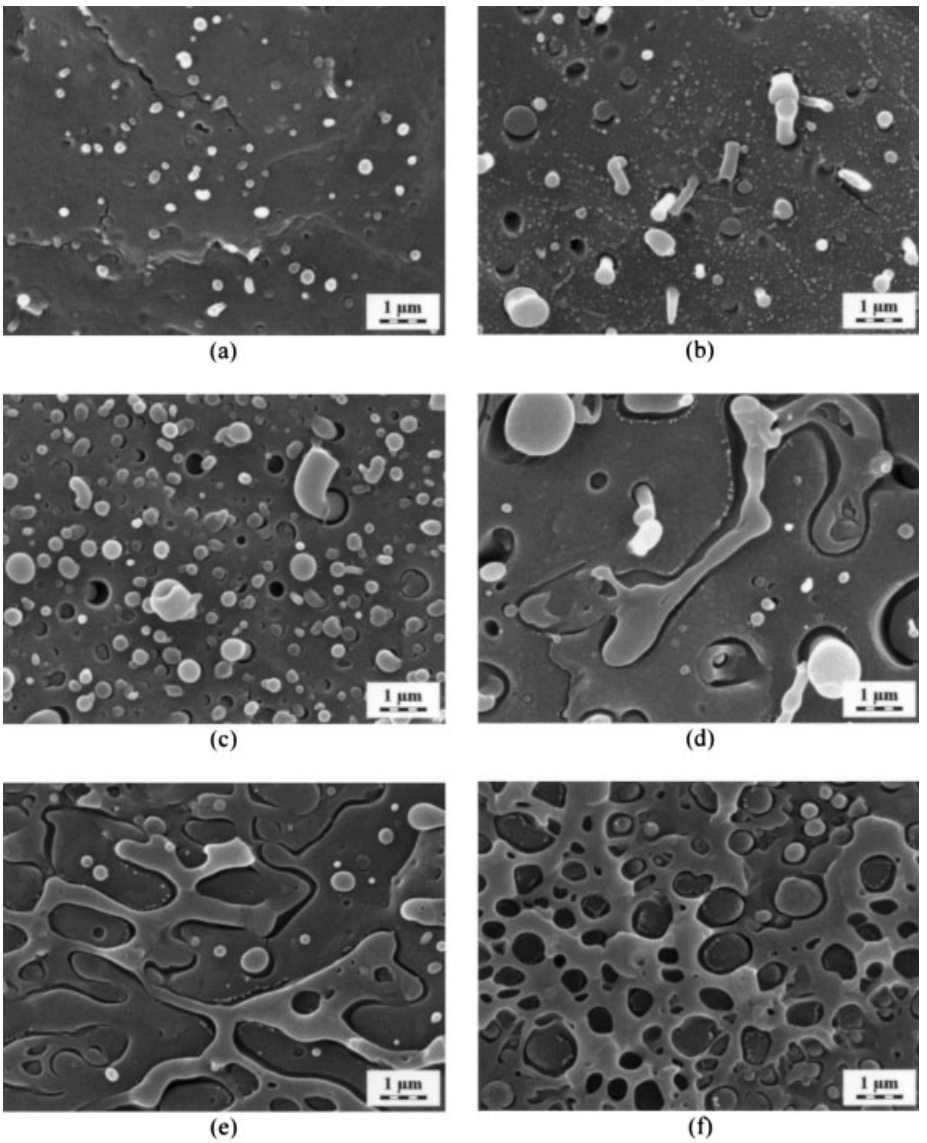

Figure 1 SEM micrographs of the fractured surfaces of PP/COC blend at six different compositions: (a) 90/10, (b) 80/20, (c) 70/30, (d) 60/40, (e) 50/50, and (f) 25/75. Fractured surfaces are perpendicular to the injection direction.

a strain gauge extensometer (Instron, model 2620; gauge length 25 mm) on ASTM dumbbell-shaped specimens tested up to 1% strain at a crosshead speed of 1 mm/min. Three specimens were tested for each blend.

Tensile creep measurements

Tensile creep was measured by using a simple apparatus equipped with a mechanical stress amplifier (lever) 10 : 1. Tests in the interval of 0.1–100 min were performed at room temperature (i.e., 21–23°C). Mechanical preconditioning consisted of applying a stress (for 1 min) which produced a strain larger than the expected final strain in the intended experiment; the following recovery (before the recorded creep was initiated) was about 1 h. Specimen dimensions were the initial distance between grips of 90 mm, cross section 10 × 4 mm. The length of creeping specimens was measured with the accuracy of 2 μm (i.e., about 0.002%).

RESULTS AND DISCUSSION

Phase morphology

Figure 1 shows SEM micrographs of fracture surfaces of PP/COC blends taken perpendicular to the injection direction. The PP/COC blends with compositions of 90/10, 80/20, 70/30, and 60/40 contain dispersed COC component in the PP matrix. In the 90/10, 80/20, and 70/30 blends, COC forms single fibers, most of

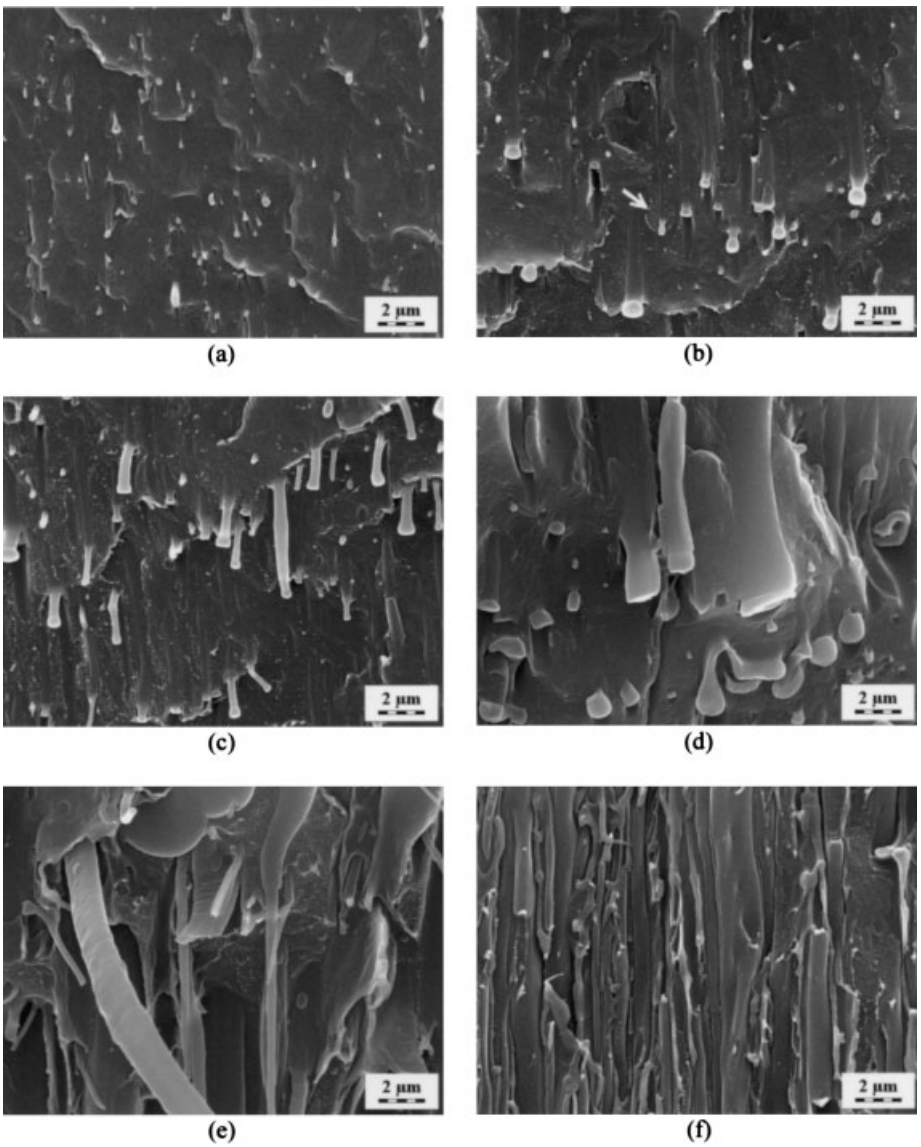

Figure 2 SEM micrographs of the fractured surfaces of PP/COC blend at six different compositions: (a) 90/10, (b) 80/20, (c) 70/30, (d) 60/40, (e) 50/50, and (f) 25/75. Fractured surfaces are parallel to the injection direction. The injection direction in all micrographs is from top to bottom. The white arrow in (b) shows plastic deformation of the PP matrix close to the broken COC fiber.

which are partly pulled out from the PP matrix. However, some COC fibers are broken at the level of fracture surface and so we can infer that there exists some interfacial adhesion between PP and COC. In other words, at least some COC fibers are long enough to be broken instead of being pulled out from the PP matrix at existing interfacial adhesion. In the 60/40 blend [Fig. 1(d)], COC tends to be partially cocontinuous and forms both fibers and larger particles of irregular shape. All COC entities are elongated in the injection direction, as confirmed by Figure 2(d). Some larger COC particles contain PP fibers, as confirmed by Figure 3(c). The 50/50 blend [Fig. 1(e)] is composed of the cocontinuous phase of PP containing COC fibers and the cocontinuous phase of COC containing PP fibers. The 25/75 blend (Fig. 1f) contains PP fibers in the COC matrix. The fibrous structure of PP in this blend is not obvious from Figure 1(f), but it is readily revealed in Figure 2(f).

Very small white spots, which are clearly seen in Figure 1(b, d, e), were probably created by local overheating during the fracture. It has been shown[27] that fracture processes in polymer specimens may increase the temperature by 300 K. This interpretation is supported by three experimental facts: (1) On fracture surfaces perpendicular to the injection direction, the white spots on the PP matrix (i.e., plastic deformations) were observed only in some regions, whereas other regions were completely smooth. (2) On fracture surfaces parallel to the injection direction (Fig. 2), the

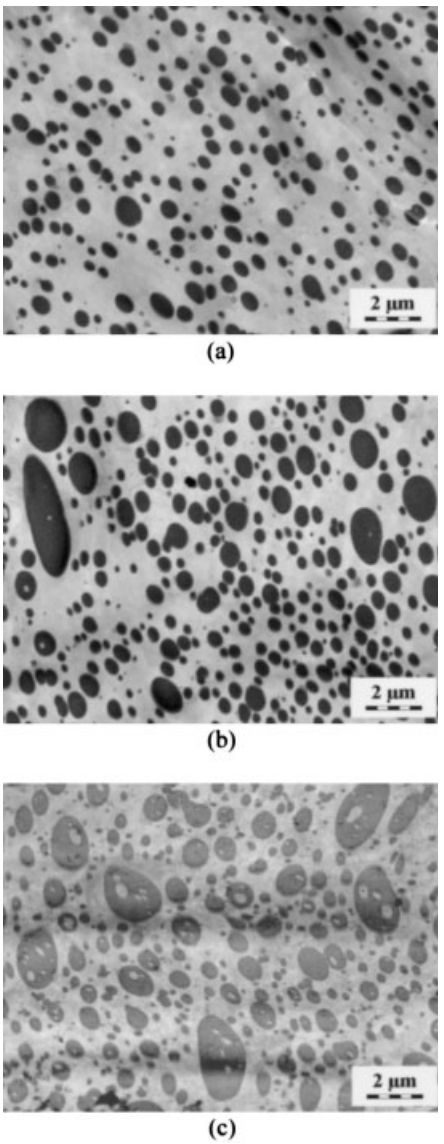

Figure 3 STEM micrographs of RuO_4-stained ultrathin sections of PP/COC blend at three different compositions: (a) 80/20, (b) 70/30, and (c) 60/40. The sections are perpendicular to the injection direction.

deformations of the PP matrix were observed in the regions close to the broken COC fibers. An example is indicated in Figure 2(b) with the white arrow. (3) The white spots occur in groups in some small regions. If the white spots were COC particles, they should be seen as black spots on STEM micrographs of RuO_4-stained ultrathin sections (Fig. 3). However, no such groups of small black spots were observed on STEM micrographs.

Figure 2 shows SEM micrographs of fracture surfaces of PP/COC blends parallel to the injection direction. It confirms that the 90/10, 80/20, and 70/30 blends contain relatively long COC fibers that are all oriented in the injection direction. Both the COC fibers and the larger COC entities in the 60/40 blend [Fig. 2(d)] and cocontinuous components in the 50/50 blend [Fig. 2(e)] show strong orientation in the injection direction as well. The SEM micrograph of the 25/75 blend [Fig. 2(f)] confirms that also the "inverted" blend contains fibers of the minority component in the matrix of the majority component.

As mentioned above, the blends were prepared with the intention to enhance mechanical properties of PP by the addition of COC. From the point of view of possible application of PP/COC blends, the blends with PP matrix and COC fibers are the most peculiar and interesting ones. That is why STEM micrographs of RuO_4-stained ultrathin sections of the 80/20, 70/30, and 60/40 blends were investigated to confront them with the SEM analysis. STEM micrographs (Fig. 3) allow us to confirm previous findings: (1) COC as the minority component forms fibers so that "classical" three-dimensional cocontinuous structure cannot be observed in the 60/40 blend; (2) the average diameter of fibers increases in the with increasing fraction of COC (Table I); (3) larger COC entities in the 60/40 blend contain thin fibers of PP (diameters around 0.15 μm).

STEM micrographs show two features worth mentioning: (1) STEM micrographs display black COC entities in white PP matrix. This means that COC is stained more intensively with ruthenium tetraoxide than PP, which can be explained as follows: ruthenium tetraoxide stains both PP and PE (polyethylene), but PE is stained faster and stronger than PP.[26] As COC contains 70% of ethene, it is stained more intensively than PP. (2) The cross sections of the fibers on SEM micrographs (Fig. 1) are circular, whereas some cross sections of the fibers on STEM micrographs (Fig. 3) are slightly elliptical. This small discrepancy is probably caused either by strong deformations acting on polymer materials during ultramicrotoming[28] or by the fact that the ultrathin sections were not exactly perpendicular to the injection direction.

Fiber diameters of the dispersed component are summarized in Table I. Each blend is characterized by

TABLE I
Diameters of the Fibers of the Minority Component in the Matrix of the Majority Component in PP/COC Blends

PP/COC composition	Fiber diameter [μm]		
	Minimum	Maximum	Average
90/10	0.1	0.4	0.25
80/20	0.1	1.0	0.55
70/30	0.1	1.5	0.8
60/40	0.1	5.1	2.6
50/50	Cocontinuous phase structure		
25/75	0.2	1.4	0.8

Note. Average fiber diameter was calculated as $1/2 \times$ (minimum + maximum).

three values (i.e., the minimum, maximum, and average fiber diameter instead of complete distribution of fiber diameters). As the distribution of fiber diameters slightly varies from place to place within each sample, the three average values of the fiber diameters seem to be more reasonable in this case. In the 90/10, 80/20, 70/30, and 60/40 blends, the minimum fiber diameter remains the same, whereas maximum and average fiber diameters increase, which means that in this composition range the fiber diameter distribution broadens but the thin fibers are found even in the 60/40 blend. Even the 50/50 blend with cocontinuous phase structure contains thin fibers of both components, with minimum diameters of approximately 0.1 μm. Diameters of PP fibers in the reverse 25/75 blend are comparable with those in the 80/20 and 70/30 blends.

Fiber lengths could not be determined precisely either from SEM micrographs or from STEM micrographs. In SEM micrographs showing fracture surfaces parallel to the injection direction (Fig. 2), the fibers emerge, break, and immerge in the matrix so that a single fiber is never observed along all its length. In STEM micrographs showing ultrathin sections parallel to the injection direction, the whole fibers would be observable only if the ultrathin sections were exactly parallel to the fibers, which is very difficult to achieve. Moreover, it would probably be impossible to prove that the ultrathin sections were really parallel to the injection direction. However, careful inspection of SEM micrographs suggests that in the 80/20, 70/30, 60/40, 50/50, and 25/75 blends the length of the fibers is at least 20 times higher than their diameter. In the 90/10 blend, the fibers are not observed so clearly but it seems that the fibers are at least 10 times longer than they are wide.

Modulus of PP/COC blends

The prepared PP/COC blends with weight fraction of COC lower than 0.4 have a structure resembling composites with uniaxially oriented short fibers, whose aspect ratio A, however, can hardly be estimated from available micrographs. Thus, well-known models for the modulus of fiber composites can be attempted to evaluate the aspect ratio of reinforcing fibers. Tensile modulus E_c in the direction of short fibers is routinely calculated[29,30] by means of the Halpin–Tsai equation:

$$E_c = E_m(1 + AB\nu_f)/(1 - B\nu_f) \quad (1)$$

where $A = 2L/d$ stands for the ratio of fiber length L and diameter d, $B = [(E_f/E_m) - 1]/[(E_f/E_m) + A]$ depends on the tensile modulus of the fibers (subscript f) and of the matrix (subscript m), and v_f is the volume fraction of fibers. For high aspect ratios, eq. (1) is reduced to the rule of mixtures (i.e., the dependence of E_c on v_f is linear):

$$E_c = E_m\nu_m + E_f\nu_f \quad (2)$$

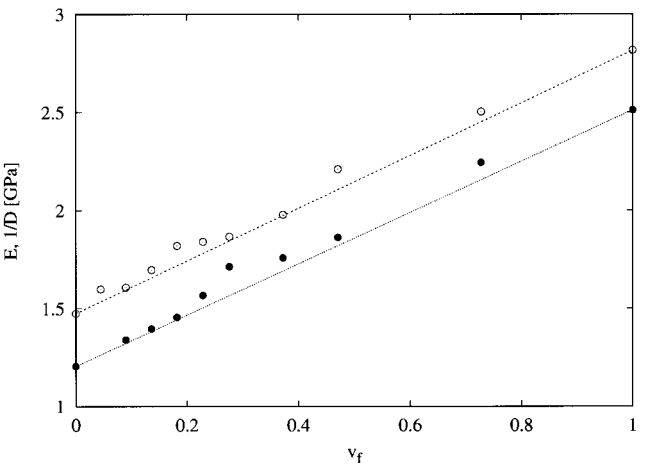

Figure 4 Tensile modulus E and the reciprocal value of tensile compliance D (measured after 1 min of creeping) of PP/COC blends as a functions of volume fraction v_f of COC component. White circles stand for values of E obtained from stress–strain measurements; black circles stand for values of $1/D$ obtained from tensile creep measurements.

Figure 4 indicates that experimental data [i.e., the tensile modulus E_c and the reciprocal value of tensile compliance D_c(1 min) measured after 1 min of creeping] are quite well fitted by eq. (2). In the case of low aspect ratios, experimental data would lie below the straight line. The difference between E and $1/D$(1 min) is caused by a different time scale of the experiments. Thus, it seems that COC fibers have a rather high aspect ratio (at least 20–30), which is in conformity with rough estimates based on SEM analysis.

CONCLUSION

PP/COC blends prepared by injection molding exhibit fibrillar morphology in a wide range of compositions, which was proven by SEM analysis of fracture surfaces and confirmed by both stress–strain and tensile creep measurements. In the 90/10, 80/20, and 70/30 blends, the PP matrix contains the COC fibers, whose average diameter increases with the increasing COC fraction. In the 60/40 blend, the COC minority component forms both fibers and larger elongated entities with PP fibers inside. The increase in fiber diameters in the 90/10, 80/20, 70/30, and 60/40 blends accords with theoretical assumptions and was confirmed by STEM analysis of RuO_4-stained ultrathin sections. The 50/50 blend contains a cocontinuous COC component with PP fibers and a cocontinuous PP component with COC fibers. The 25/75 blend contains

the PP fibers in the COC matrix. In all blends, the fibers are oriented in the injection direction and act as a reinforcing component, which was proven by stress-strain and creep measurements. The fiber aspect ratio was estimated to be at least 20, by using both SEM micrographs and experimentally assessed values of elastic moduli.

Current literature[15–25] indicates increasing interest in heterogeneous polymer blends with cocontinuous components (phases). For instance, gas permeability of blends starts to rise as soon as the component with substantially higher permeability assumes partial continuity.[31] In the case of mechanical properties,[15–20] a cocontinuous upgrading component can impart to blends higher modulus, yield strength, resistance to creep, etc. The effects of this component would be even higher, if it could assume the form of fibers. However, it should be noted that ordinary polymer blends are isotropic materials, while structures with fibers usually rank among orthotropic or quasi-isotropic materials.[29,30] Thus, a number of attempts have been made to prepare blends with a fibrous[32–41] reinforcing component. However, to this end, liquid crystalline polymers (LCP),[32–34] extensive tensile deformation (drawing) as the last operation in processing cycle,[35–39,41] or other specific treatments of the samples (such as shear deformation[40]) were mostly employed. Thus, our PP/COC blends with spontaneously formed COC fibers seem to be materials with exceptional structure. COC fibers with a high aspect ratio may not have been a product of additional drawing only; it may be assumed that the COC fibers had already been formed during mixing and preserved in the subsequent process of injection molding. The latter process probably brought about uniaxial orientation and further elongation of already present COC fibers. Unfortunately, it was not possible to systematically vary conditions of blend processing to specify how they affect produced morphology (cf. ref. 33). Thus, the described structure was probably obtained thanks to the serendipity in selecting parent polymers and adjusting processing conditions.

This work was supported through Grant 106/02/P029 awarded by the Grant Agency of the Czech Republic; Grant A4050105 awarded by the Grant Agency of the Academy of Sciences of the Czech Republic, and by the Academy of Sciences of the Czech Republic (Project AVOZ 4050913). The authors thank Ticona, Frankfurt, Germany for providing COC polymer; Basell, Ferrara, Italy for providing PP polymer; and Dr. P. Goberti for preparation of blends and test specimens.

References

1. Tritto, I.; Boggioni, L.; Jansen, J. C.; Thorshaug, K.; Sacchi, M. C.; Ferro, D. R. Macromolecules 2002, 35, 616.
2. Thorshaug, K.; Mendichi, R.; Boggioni, L.; Tritto, I.; Trinkle, S.; Friedrich, C.; Muelhaupt, R. Macromolecules 2002, 35, 2903.
3. Khanarian, G. Polym Eng Sci 2000, 40, 2590.
4. Huang, W. J.; Chang, F. C.; Chu, P. J. J. Polymer 2000, 41, 6095.
5. Chu, P. J. J.; Huang, W. J.; Chang. F. C. Polymer 2001, 42, 2185.
6. Scrivani, T.; Benavente, R.; Perez, E.; Perena, J. M.; Macromol Chem Phys 2001, 202, 2547.
7. Forsyth, J.; Perena, J. M.; Benavente, R.; Perez, E.; Tritto, I.; Boggioni, L.; Brintzinnger, H. H. Macromol Chem Phys 2001, 202, 614.
8. Forsyth, J.; Scrivani, T.; Benavente, R.; Marestin, C.; Perena, J. M. Appl Polym Sci 2001, 82, 2159.
9. Topas (COC); booklet; Ticona: Hoechst, Germany, 1995.
10. Rana, D.; Lee, C. H.; Cho, K.; Lee, B. H.; Choe, S. J Appl Polym Sci 1998, 69, 2441.
11. Luettmer-Strathmann, J.; Lipson, J. E. G. Macromolecules 1999, 32, 1093.
12. Ivanov, I.; Muke, S.; Kao, N.; Bhattacharya, S. N. Polymer 2001, 42, 9809.
13. Cimino, S.; DiPace, E.; Karasz, F. E.; Martuscelli, E.; Silvestre, C. Polymer 1993, 34, 972.
14. DiLiello, V.; Martuscelli, E.; Ragosta, G. J Mater Sci 1989, 24, 3235.
15. Kolařík, J. Polym Eng Sci 1996, 36, 2518.
16. Horák, Z.; Kolařík, J.; Šípek, M.; Hynek, V.; Večerka, F. J Appl Polym Sci 1998, 69, 2615.
17. Kolařík, J.; Pegoretti, A.; Fambri, L.; Penati, A. J Polym Res 2000, 7, 7.
18. Kolařík, J.; Fambri, L.; Pegoretti, A.; Penati, A. Polym Adv Technol 2000, 11, 75.
19. Kolařík, J.; Fambri, L.; Pegoretti, A.; Penati, A. Polym Eng Sci 2002, 42, 161.
20. Kolařík, J.; Pegoretti, A.; Fambri, L.; Penati, A. J Appl Polym Sci, to appear.
21. Matsuoka, T.; Yamamoto, S. J Appl Polym Sci 1998, 68, 807.
22. Willemse, R. C.; de Boer, A. P.; van Dam, J.; Gotsis, A. D. Polymer 1998, 39, 5879
23. Willemse, R. C. Polymer 1999, 40, 2175.
24. Veenstra, H.; Van Dam, J.; de Boer, A. P. Polymer 1999, 40, 1190.
25. Veenstra, H.; Verkooijen, P. C. J.; van Lent, B. J. J.; Van Dam, J.; de Boer, A. P.; Nijhof, H. J. Polymer 2000, 41, 1817.
26. Brown, G. M.; Butler, J. H. Polymer 1997, 38, 3937.
27. Fox, P. G.; Fuller, K. N. G. Nat Phys Sci 1971, 234, 13.
28. Lednicky, F.; Hromadkova, J.; Pientka, Z. Polymer 2001, 42, 4329.
29. Ashton, J. E.; Halpin, J. C.; Petit, P. H. Primer on Composite Materials, Analysis; Technomic: Stamford, 1969.
30. Agarwal, B. D.; Broutman, L. J. Analysis and Performance of Fiber Composites; Wiley-Interscience: New York, 1980.
31. Kolařík, J. Polym Eng Sci 2000, 40, 127.
32. Verhoogt, H.; Langelaan, H. C.; Van Dam, J.; De Boer, A. P. Polym Eng Sci 1993, 33, 754.
33. Machiels, A. G. C.; Denys, K. F. J.; Van Dam, J.; De Boer, A. P. Polym Eng Sci 1996, 36, 2451.
34. Machiels, A. G. C.; Denys, K. F. J.; Van Dam, J.; De Boer, A. P. Polym Eng Sci 1997, 37, 59.
35. Monticciolo, A.; Cassagnau, P.; Michel, A. Polym Eng Sci 1998, 38, 1882.
36. Evstatiev, M.; Schultz, J. M.; Fakirov, S.; Friedrich, K. Polym Eng Sci 2001, 41, 192.
37. Boyaud, M. F.; Cassagnau, P.; Michel, A. Polym Eng Sci 2001, 41, 684.
38. Ling, Z.; Rui, H.; Liangbin, L.; Gang, W. J Appl Polym Sci 2002, 83, 1870.
39. Tzur, A.; Narkis, M.; Siegmann, A. J Appl Polym Sci 2001, 82, 661.
40. Deyrail, Y.; Fulchiron, R.; Cassagnau, P. Polymer 2002, 43 3311.
41. Li, Z. M.; Yang, M. B.; Huang, R.; Yang, W.; Feng, J. M. Polym-Plast Technol Eng 2002, 41, 19.